# The Influence of Native Oxide Layers of InP on the Shape of Etching Profiles at Resist Edges

**P. H. L. Notten**

*Philips Research Laboratories, 5600 JA Eindhoven, The Netherlands*

ABSTRACT

Profile etching experiments made on InP in solutions of $Br_2$-HBr revealed that the profile shape is strongly dependent on the resist orientation and on whether $SiO_2$ or photoresist is used as a mask. It was found that the local etch rate of the (111)In crystallographic planes can be significantly enhanced near the resist edges. In the extreme case the dissolution rate was found to be controlled by $Br_2$ diffusion in solution which resulted in rounded profiles. A model is proposed which can account for this apparently anomalous etching behavior. The anisotropic etching of thin surface layers is essential in this model. Experimental results can be explained if it is assumed that native oxide layers covering the monocrystalline InP substrates play this role. The local etching kinetics of crystallographic facets and, consequently, the profile shape are strongly determined by the lateral etch rate of these oxide layers.

InP devices are widely used in optical telecommunication systems (1). Etching of special predetermined forms is an essential step in the production of these devices. Recently, we have shown that the shape of III-V semiconductor profiles near resist edges depends not only on the dissolution kinetics of individual crystallographic planes but also on the dissolution mechanism (2, 3). It was concluded that, due to the formation of a native oxide layer, electroless etching systems generally cannot be applied to dissolve InP. This was attributed to the fact that transfer of free charge carriers from an oxidizing agent in solution to the semiconductor is strongly inhibited by the oxide. On the other hand, chemical etchants were found to be more appropriate, as these solutions dissolve both the oxide and the underlying InP substrate [Table 7.1 of (3)]. One of these chemical etching systems, *viz.*, the $Br_2$-HBr system, was investigated in detail in previous work (2-4). On the basis of this work it was concluded that the macroscopic etching kinetics of various crystallographic faces is, in many cases, a good guideline in predicting the profile shape near resist edges. However, anomalous etching results were obtained under certain experimental conditions which shows that the macroscopic and local, "microscopic," etching kinetics may be quite different. This leads us to conclude that factors other than those determining the macroscopic etching kinetics may contribute to dissolution near the resist edges. The aim of the work described in this paper is to determine these factors. The etching behavior of the InP/$Br_2$-HBr system at resist edges was therefore investigated in more detail. The influence of both the nature of the resist and the resist orientation on the profile shape was examined. In addition, the temperature dependence of the etching process was investigated.

In previous works bromine was found to be the active etching species in the above system (2-4). Since the partial vapor pressure of $Br_2$ is large in aqueous solutions an excess of $Br^-$ was added to the etchant to complex $Br_2$, mainly leading to $Br_3^-$. Stable solutions are obtained in this way. However, to reduce the contribution of etching by HBr, which is also a chemical etchant for InP in its undissociated form (2), the HBr concentration should not exceed 5 molar (3, 4). An 0.1*M* $Br_2$ and 4.5*M* HBr solution was therefore used as etchant in the present work.

## Experimental

The zinc-doped InP slices were obtained from liquid-encapsulated Czochralski material which was grown at this laboratory. The carrier concentration was in the range of 1-2 $\times$ $10^{18}$ $cm^{-3}$. The (001) oriented InP crystals were mechano-chemically polished in a methanol solution containing 0.1*M* $Br_2$ (5).

To perform the profile etching experiments the (001) surfaces of the crystals were partly covered with a resist layer. Two different patterns were used. For one series of experiments we covered only half of the crystal surface with resist which we denote as the semi-infinite case. For another series, a masking pattern with variable slit width ($a$) was used (see Fig. 1). The widths used were $a$ = 1, 3, 10, 30, 100, 300 to 1000 μm. The unmasked stripes in the resist pattern were aligned in two directions as shown in Fig. 1, perpendicular to the two planes which can be very easily cleaved, *i.e.*, the (110) and ($\bar{1}$10) planes (5). Either an $SiO_2$ layer or a photoresist layer was used as masking material. The $SiO_2$ resists which were produced with conventional CVD technology at an operating temperature of 400°C, had a thickness ($d_r$) of about 100 nm. The photoresist (HPR-204) was obtained from Hunt. Thin photoresist layers at the surface were made by spinning the wafers at 6000 rpm at room temperature. The resist patterns were produced by standard photolithographic techniques and were baked for 30 min at 120°C. The mask preparation procedures were performed in a "clean room." The orientation accuracy was determined by a microscope and was better than 0.05°. The samples were about 6 $\times$ 6 mm large and were mounted on a glass plate before etching.

The glass plate with the sample was placed horizontally in a closed vessel containing the etching solution. The vessel was surrounded by a waterjacket to allow the etching solution to be thermostated at various temperatures (accuracy, ±0.5°C). The temperature range at which the etching experiments were performed was between −10° and +40°C. To cool down the etchants a cryostat (PBC-4 bath cooler from Neslab Instruments, Incorporated) was used in combination with the thermostat. The etching experiments were performed in the dark. All solutions were prepared from reagent grade chemicals [100% bromine (~20 molar) and 47% hydrobromic acid (~9 molar)] and were di-

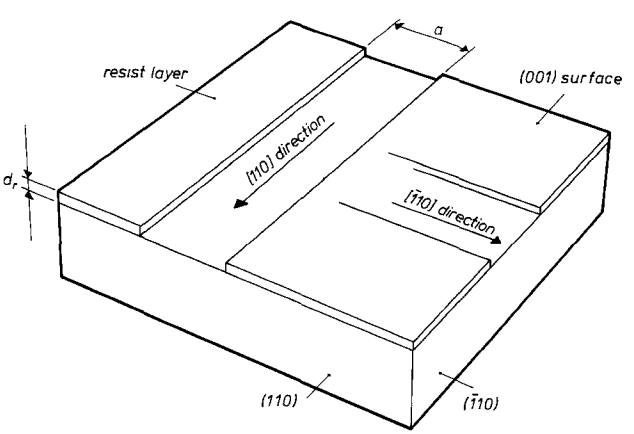


**Fig. 1. Resist orientation in two directions at right angles on the (001) semiconductor surface. The resist edges are aligned either in the [110] or [$\bar{1}$10] direction, perpendicular to the (110) and ($\bar{1}$10) cleave faces, respectively. The resist thickness is represented by $d_r$ and the slit width by $a$. The width is varied between 1 μm and semi-infinite.**

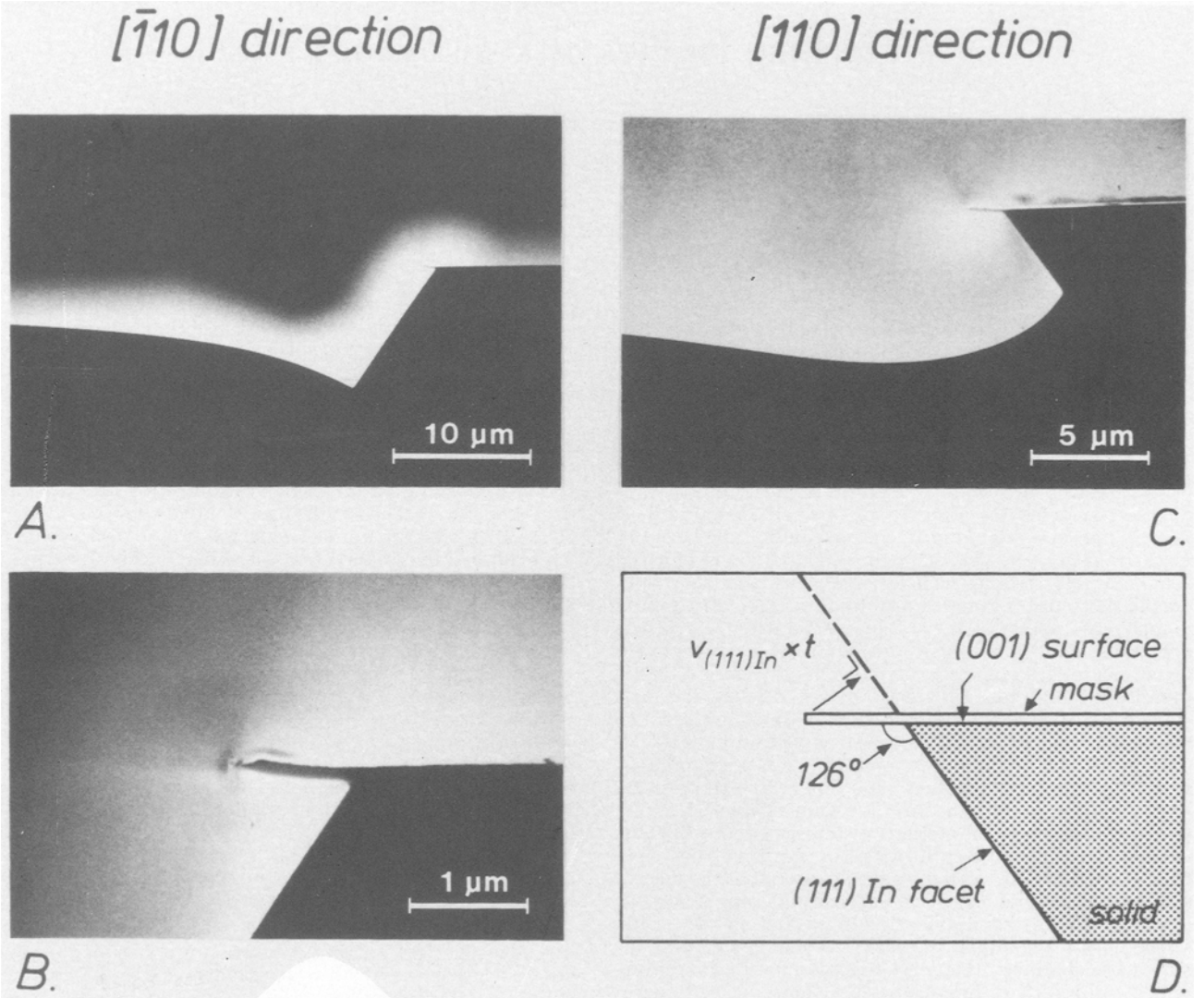


**Fig. 2. SEM photographs of profiles after 7.5 min etching in a solution of 0.1M $Br_2$, 4.5M HBr. The crystals were covered with a semi-infinite $SiO_2$ mask. The profile shown in A was obtained with the resist aligned in the [$\bar{1}$10] direction at an etching temperature of 20°C. A higher magnification of the same profile in the resist-edge region is shown in B. Profile C was etched with the resist oriented in the [110] direction at a temperature of 0°C. The etch rate of the (111)In facet in the [110] direction is defined in D.**

luted with deionized water. After etching, the slices were cleaved perpendicular to the resist edge and the etched profiles were examined in a scanning electron microscope (SEM).

## Results

Profile etching experiments were performed in a solution of 0.1*M* $Br_2$ and 4.5*M* HBr at various temperatures. The surface was masked with a semi-infinite $SiO_2$ layer aligned in either the [$\bar{1}$10] direction or the [110] direction. The semiconductor was etched for 7.5 min at a temperature between −8° and +40°C. Typical examples of etched profiles obtained with the resist in the two directions are shown in Fig. 2. The profile obtained in the [$\bar{1}$10] direction at a temperature of 20°C is shown in Fig. 2A. A facet is clearly revealed near the resist edge. This indicates that the etch rate of the facet is kinetically controlled. The faceted edge makes an angle of 54° with the (001) surface and is thus attributed to the (111)In plane (6), the same face whose macroscopic etch rate was also found to be kinetically controlled (2-4). As defined in the previous works the etch rate of this facet [$v_{(111)In}$] can be obtained from its displacement with respect to the resist edge and the etching time. To obtain an accurate estimate of the etch rate a higher magnification of the corner region of the same profile was used (Fig. 2B).

Curve (a) of Fig. 3 shows the dependence of the etch rate of the (111)In facet on the temperature in an Arrhenius plot for [$\bar{1}$10] alignment of the resist layer. The logarithm of $v_{(111)In}$ is linearly dependent on the reciprocal of the temperature. From the slope of this line an activation energy of $41 \times 10^3$ J · $mol^{-1}$ is calculated. This value is typical of kinetically controlled processes (7). The agreement of the etch rate of this plane in the etched profiles and the chemical etch rate of the macroscopic plane at the same temperature as determined in (4) is excellent. The curved surface further removed from the mask (Fig. 2A) shows that the etch rate of other facets, including that of the (001) surface, is diffusion controlled. The etch depth in the vicinity of the resist edge is strongly enhanced due to two-dimensional diffusion of bromine species in solution. This is in accordance with the reported mathematical models (8, 9).

A typical example of a profile obtained in the [110] direction at 0°C is shown in Fig. 2C. In this case the facet makes an angle of approximately 126° with the overhanging resist layer. Since the resist edge is aligned in the [110] direction, crystallographic considerations lead us to conclude that a (111)In facet has again been exposed (6, 10). The etch rate of the (111)In facet can also be obtained from its displacement with respect to the resist edge and the etching time, as shown schematically in Fig. 2D. Curve (b) of Fig. 3 reveals a linear dependence of the logarithm of this etch rate on $T^{-1}$ in the temperature range −8° to +20°C. This line has the same slope as curve (a) of this figure. It is, however, strange that the etch rate of the (111)In plane in the [$\bar{1}$10] direction is about five times higher than that in the [$\bar{1}$10] di-

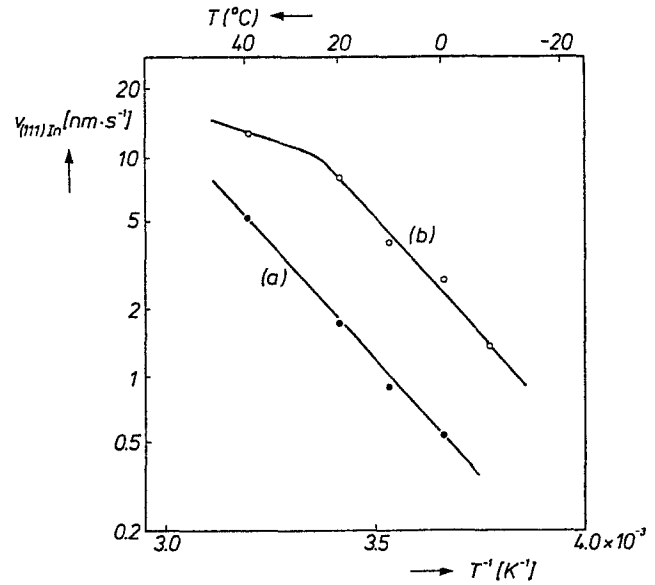


**Fig. 3. The local etch rate of the (111)In plane, as obtained from profile etching experiments performed with a semi-infinite $SiO_2$ mask as a function of the reciprocal temperature. The same etchant was used as in Fig. 2. The etching time was 7.5 min. Curve (a): the $SiO_2$ mask aligned in the [$\bar{1}$10] direction; curve (b): alignment in the [110] direction.**

rection in the corresponding temperature range [compare curves (a) and (b) of Fig. 3]. This is even more surprising since the local etch rates in curve (a) agree with the reported macroscopic etch rate (4).

A deviation from the straight line is found at 40°C [see Fig. 3 curve (b)]. This must be attributed to the fact that etching of the (111)In facet is no longer kinetically controlled but has become diffusion controlled. Indeed, at this temperature a rounded profile is obtained in the [110] direction, without any facet as one would expect (8, 9). The temperature dependence of the etch rate is significantly lower under these diffusion-controlled conditions, which is indicated by a decreased slope in the Arrhenius plot [curve (b) of Fig. 3]. This is in agreement with the considerations given by Mori and Watanabe (7). That a gradual transition from kinetically controlled to diffusion-controlled etching occurred in this temperature range could also be deduced from the fact that, on going from lower to higher temperature, the length of the (111)In facet in the profiles strongly decreased, ultimately disappearing at the highest temperature. This is not observed with the profiles in the [$\bar{1}$10] direction.

Etching experiments were also performed at various temperatures using a photoresist layer as a mask. The slit width was varied between 1 and 1000 μm. The resist layers were aligned in both the [$\bar{1}$10] and [110] directions. For comparison the same experiments were performed with crystals masked with $SiO_2$. Typical examples of profiles etched for 7.5 min through a 10 μm slit at a temperature of 20°C are shown in Fig. 4. The results obtained with the $SiO_2$ resist in both directions (Fig. 4A and B) are similar to those shown in Fig. 2 where a semi-infinite resist pattern was used. The etch rate of the (111)In facet in the [$\bar{1}$10] direction (Fig. 4A) agrees with the macroscopic etch rate. In the [110] direction (Fig. 4B) the etch rate is significantly enhanced [compare also curves (a) and (b) of Fig. 3].

Results obtained with photoresist layers in the [$\bar{1}$10] direction show a V-groove shape (Fig. 4C), similar to that found with the $SiO_2$-resist in the corresponding orientation (compare with Fig. 4A). Here too, a linear dependence of $\log v_{(111)In}$ on $T^{-1}$ was observed. The line has the same slope as found before in curve (a) of Fig. 3, thus indicating that the dissolution rate of the (111)In facet is kinetically controlled. It should, however, be noted that the etch rate of the (111)In face in the photoresist case is significantly higher than that found with $SiO_2$ resist (compare Fig. 4A and C). Strikingly, the profiles found in the [110] direction did not reveal any crystallographic facet (Fig. 4D). In contrast to the result found with $SiO_2$ in the corresponding resist orientation, rounded profiles are observed (compare Fig. 4B and D). These profiles were observed not only at 20°C but even at very low temperatures ($-10° < T < 20°C$). A plot of the logarithm of the underetch rate as a function of the reciprocal temperature also yields a straight line. However, the slope of this line is much lower than that found for kinetically controlled reactions. This is expected for a diffusion-controlled process (7). From the slope, an activation energy of $15 \times 10^3$ J · mol$^{-1}$ is calculated. Similar etching results as those described above were also found with other slit widths.

It is well-known that native oxide layers which are always present at the surface of III-V semiconductors (11), may have a considerable thickness in the case of InP. Several authors (12-14) attributed changes in the shape of profiles at InP to changes in both the thickness and the nature of the thermally grown oxide layers. The shape of the profiles was found to be dependent on the temperature and on the conditions under which the various oxide layers were formed. The fact that the etching profiles are strongly dependent on whether an $SiO_2$ layer or a photoresist layer is used suggests that the resist induces changes in the morphology of the oxide.

In order to investigate the effect of a native oxide film at InP on the microscopic etching kinetics, etchants are required which can dissolve the oxide below resist layers selectively with respect to the InP substrate. HBr solutions were found to be appropriate for this purpose. A 4.5*M* HBr solution was used at various temperatures to investigate this selectivity. Two aspects were studied: the anisotropy in the etch rate of the (111)In facet in [$\bar{1}$10] and the [110] resist orientations [see *e.g.*, curves (a) and (b) of Fig. 3] and the pronounced differences obtained with different resist layers. The results found with an $SiO_2$ resist at 40°C are shown in Fig. 5. The cross-section near the $SiO_2$ edge in the [110] direction is shown in Fig. 5A. It is obvious that the underetching is considerable. It is further noted that etching mainly occurred in the region where the resist layer was originally positioned on the InP surface. Outside this region in the unmasked area the InP has hardly been etched, as would be expected from the low macroscopic etch rate measured in HBr solutions of this composition (2-4). In contrast to the result of Fig. 5A no underetching is found in the [$\bar{1}$10] direction. This can also be seen in the top-view shown in Fig. 5B. Underetching is not found along the entire resist edge in the [$\bar{1}$10] direction. An almost constant value of 5.6 μm is found in the [110] direction, which shows that etching proceeds uniformly along the entire resist edge.

Similar results, revealing the importance of the crystal orientation, were also found with photoresist as mask. The effects at the resist/substrate interface are even more pronounced than in the $SiO_2$ case. This is illustrated in Fig. 6. A comparison between the results obtained with the masked edge in the [110] direction under identical etching conditions with a photoresist (Fig. 6A) and an $SiO_2$ resist (Fig. 6B) reveals that the lateral etch rate in the former case is approximately three times higher. As in the $SiO_2$ case, etching proceeds uniformly along the entire resist edge and is limited to the region below the mask. The etch rate of the uncovered InP outside this region is again negligibly low. It was found that the lateral etch rate in the present HBr solution depends strongly on the temperature of the etchant. However, etching stops completely below a critical temperature, around 20°-25°C.

## Discussion

A comparison between the macroscopic etching results reported in (3, 4) and the profile etching results of Fig. 2-4 clearly shows that the microscopic and macroscopic etching kinetics may be quite different. This depends on the orientation of the resist layers (Fig. 3) and also on the nature of these layers (Fig. 4). This indicates that factors other than those determining the macroscopic etching kinetics may contribute to the dissolution near resist edges.

It has been suggested by Huo *et al.* that a reduced adhesion between the resist layer and the substrate may be the

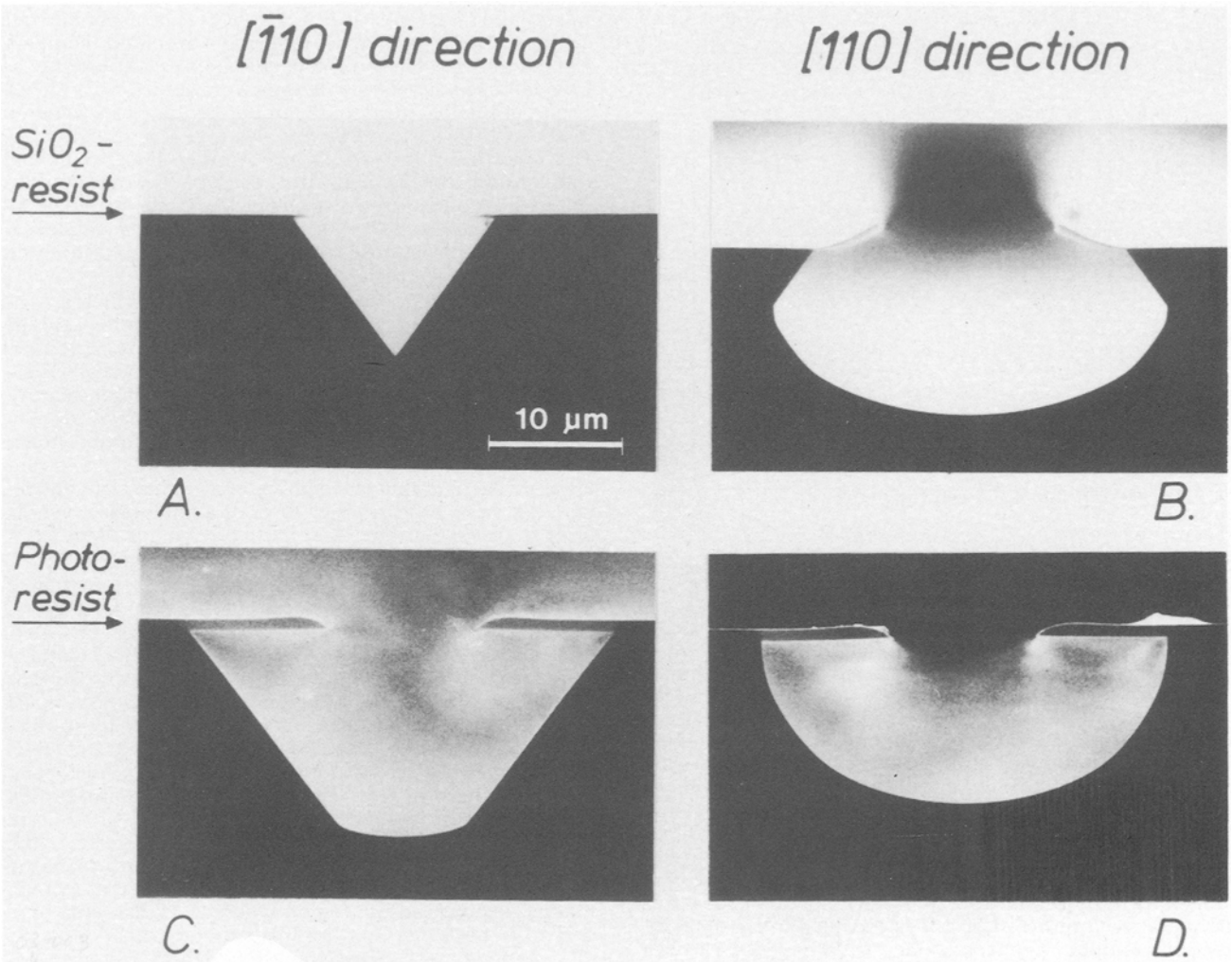


**Fig. 4. Dependence of the profile on both the type and the orientation of the resist for the InP/0.1M $Br_2$, 4.5M HBr etching system. Etching was performed at 20°C during 7.5 min and $a = 10$ μm in all cases. The results found with $SiO_2$ resist are shown in the SEM photographs A and B. Those obtained with photoresist are shown in C and D. The resist was aligned in either the [$\bar{1}$10] direction (A and C) or the [110] direction (B and D). The same magnification is used in all photographs.**

cause of the various etching profiles (14). In this respect it should be emphasized that the profiles described here are completely reproducible under a variety of etching conditions. This is also evident from the reproducible linear dependence found in the Arrhenius plots of Fig. 3. Moreover, the lack of adhesion cannot explain the anisotropy found with each resist layer in the two resist orientations. Furthermore, it has been shown that surface modifiers or primers, which function is often attributed to improve the adhesion between a substrate and a resist layer, accomplish just the opposite effect, *i.e.*, an enhancement of etch rates of crystallographic facets near the primer layer, while reduced etch rates would be expected as a result of a better adhesion (13, 14). For these reasons, it seems very likely that the different etching profiles are not due to adhesion problems.

The importance of the oxide film for etching of profiles in InP has been clearly shown by Dautremont *et al.* (12). Two important conclusions can be drawn on the basis of their work and the present etching results in HBr solutions at elevated temperatures.

In the first place, it is clear that resist layers induce changes in the native oxide as a result of which etching is initiated only in the vicinity of the resist (see Fig. 6). Since oxides have, in general, an amorphous structure (15-17), it is rather surprising that the etch rate is direction dependent (see Fig. 5B). It should, however, be kept in mind that the underlying InP is monocrystalline and that initially the oxide may grow epitaxially. That such a mechanism is realistic was recently shown by Ourmazd *et al.* (18) for Si, covered with an amorphous $SiO_2$ film. Using high resolution transmission electron microscopy, they showed that the transformation from crystalline Si to amorphous $SiO_2$ proceeds via a thin crystalline transition layer. The crystalline $SiO_2$ layer was found to have a completely different atomic structure in the [$\bar{1}$10] and [110] directions. We suggest that the thin native oxide film on InP also has an ordered crystal structure. Whether the complete oxide layer or only a thin transition region is crystalline is not important for the present discussion. The anisotropic etching behavior of the oxide layer found in the [$\bar{1}$10] and [110] directions (Fig. 5B) can be explained by assuming that the chemical resistivity is dependent on the atomic structure of the oxide.

In the second place it is clear that the type of resist influences considerably the etch rate of the oxide layer (Fig. 6). This may be attributed to differences in oxide structure. In this respect it is important to note that the procedure for applying the mask to the substrate is different for the two resists used. In particular, the considerable difference in temperature is probably important; photoresist is applied at room temperature and is subsequently baked at 120°C whereas the $SiO_2$ is deposited at 400°C. The pretreatment temperature was reported to have a significant influence on etched profiles (12-14).

It can be concluded that the dissolution rate of the crystalline top layer strongly depends on its orientation and also on the nature of the mask. It is not clear whether the top layer consists only of a crystalline oxide film or whether that part of the substrate, which might be disturbed by the pretreatment procedure, must also be considered.

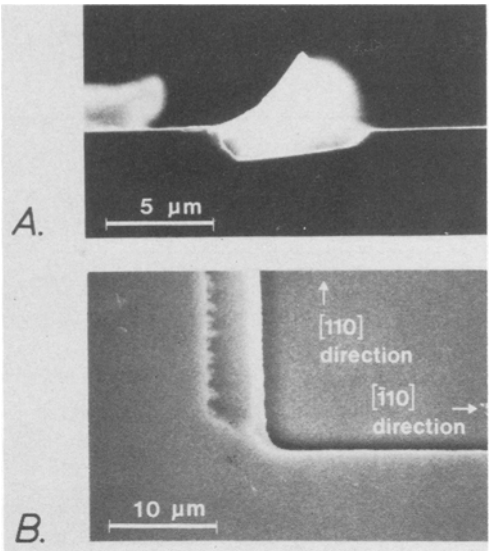


Fig. 5. Anisotropic results obtained with InP after 10 min etching in a 4.5M HBr solution at 40°C. SEM photograph A shows a cross section of the profile with the $SiO_2$ mask aligned in the [110] direction. Lateral etching only occurred in the mask-edge region; the white area below the curled resist is due to charging in the SEM. The top view (B) confirms uniform underetching for mask alignment in the [110] direction; no underetching is found with the mask edge in the [$\bar{1}$10] direction.

The influence of thin surface layers on the shape of etched profiles in isotropic materials has been reported by several authors (16, 19, 20). These materials are often intentionally covered with a thin surface film of different composition to obtain special effects. The so-called bevel or taper etching is based on the fact that the etch rate of the thin top layer covering a substrate material under the resist layer is higher than the etch rate of the substrate material in the same etchant. It has been shown that by regulating the etch rate of the top layer, either by changing the nature of this layer (15, 16) or the composition of the etchant (19, 20), the beveling angle can be adjusted between 3° and 40°. To regulate the beveling angle over such a wide range, etching of the substrate must be isotropic (15). For this reason only polycrystalline (19) and amorphous materials (15, 16, 20), very often metals (19, 20) or oxides (15, 16), can be successfully submitted to this procedure. Since the principle of bevel etching forms the basis for the explanation of the present etching results in monocrystalline materials this mechanism will now be described.

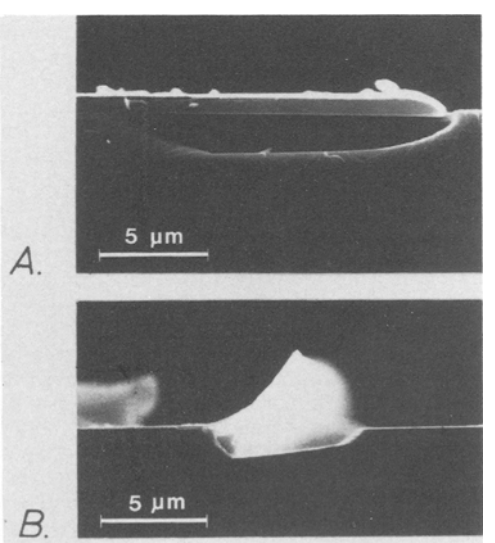


Fig. 6. The influence of the type of resist on the lateral etch rate in the mask-edge region. InP with a semi-infinite mask was etched for 10 min in a 4.5M HBr solution at 40°C. Both the photoresist (A) and the $SiO_2$ resist (B) were aligned in the [110] direction.

The bevel etching mechanism is illustrated schematically in Fig. 7 (19). Three different situations are shown. Etching of the substrate material is assumed to be kinetically controlled and isotropic, in all cases, *i.e.*, the dissolution rate is the same in all directions. When the etch rate of the surface layer (sl) is lower than that of the substrate [$v_{sl}(a) < v_{substrate}$], isotropic etching of the substrate is found [curve (a) of Fig. 7], as predicted by theory (9). When, however, the lateral etch rate of the surface layer exceeds that of the substrate [$v_{sl}(b) > v_{substrate}$], the underlying substrate is exposed and brought into contact with the etchant; dissolution of the newly formed surface results in a beveled face in the profile of curve (b). The angle this face makes with the surface is clearly dependent on the lateral etch rate of the surface layer [compare curves (b) and (c) of Fig. 7]. In this way, the bevel angle can be adjusted by regulating the etch rate of the surface layer. It should, however be emphasized that these beveled faces are not crystallographic facets.

From the above model (15, 16, 19, 20) it is clear that thin surface layers covering amorphous or polycrystalline substrates have a strong influence on the shape of profiles near resist edges. Although bevel etching is restricted to these isotropic materials, it might be expected that thin surface films could also have important implications for the etching of microscopic structures in monocrystalline materials. It is clear from the above discussion that the native oxide layers on the surface of III-V compounds can also function as a thin etchable top layer and thus influence the profiles as we will show in the following model.

We have demonstrated that the native oxide layer is dissolved at elevated temperatures in a solution of HBr (Fig. 5), a chemical etchant (3). When we assume that $Br_2$, also a chemical etchant (3), is able to etch the oxide layer even at moderate temperatures, and we further assume anisotropy of the oxide layer similar to that found with HBr, then the apparent anomaly of Fig. 4 can be explained as follows. The actual situation near the monocrystalline semiconductor surface is schematically represented in Fig. 8 A-D. Cases A-D of Fig. 8 refer to the corresponding cases of Fig. 4. The thin native oxide, between the resist layer and the lightly shaded InP substrate is represented in Fig. 8 by the dashed area. When the lateral etch rate of the oxide ($v_{ox}$) is negligibly low in the [$\bar{1}$10] direction (see Fig. 5B), it is evident that the oxide layer does not influ-

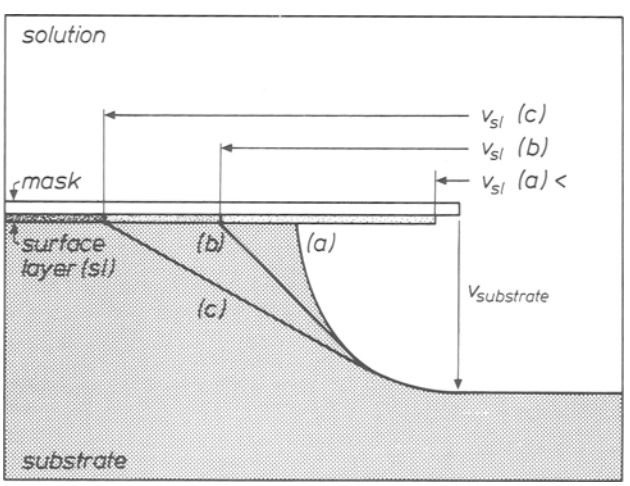


Fig. 7. Schematic representation of the bevel etching mechanism. The angle which the beveled "face" makes with the surface is dependent on the lateral etch rate of the surface layer ($v_{sl}$). The substrate is assumed to be etched isotropically at a kinetically controlled rate ($v_{substrate}$). Curve (a) shows the etch profile expected when $v_{sl}(a) < (v_{substrate})$. When $v_{sl}(b)$, $v_{sl}(c) > v_{substrate}$, the profile is changed significantly as curves (b) and (c) show. The arrows labeled $v_{substrate}$, $v_{sl}(a)$, $v_{sl}(b)$, and $v_{sl}(c)$ show the relative magnitudes of the etch rate of substrate and top layer for three different cases.

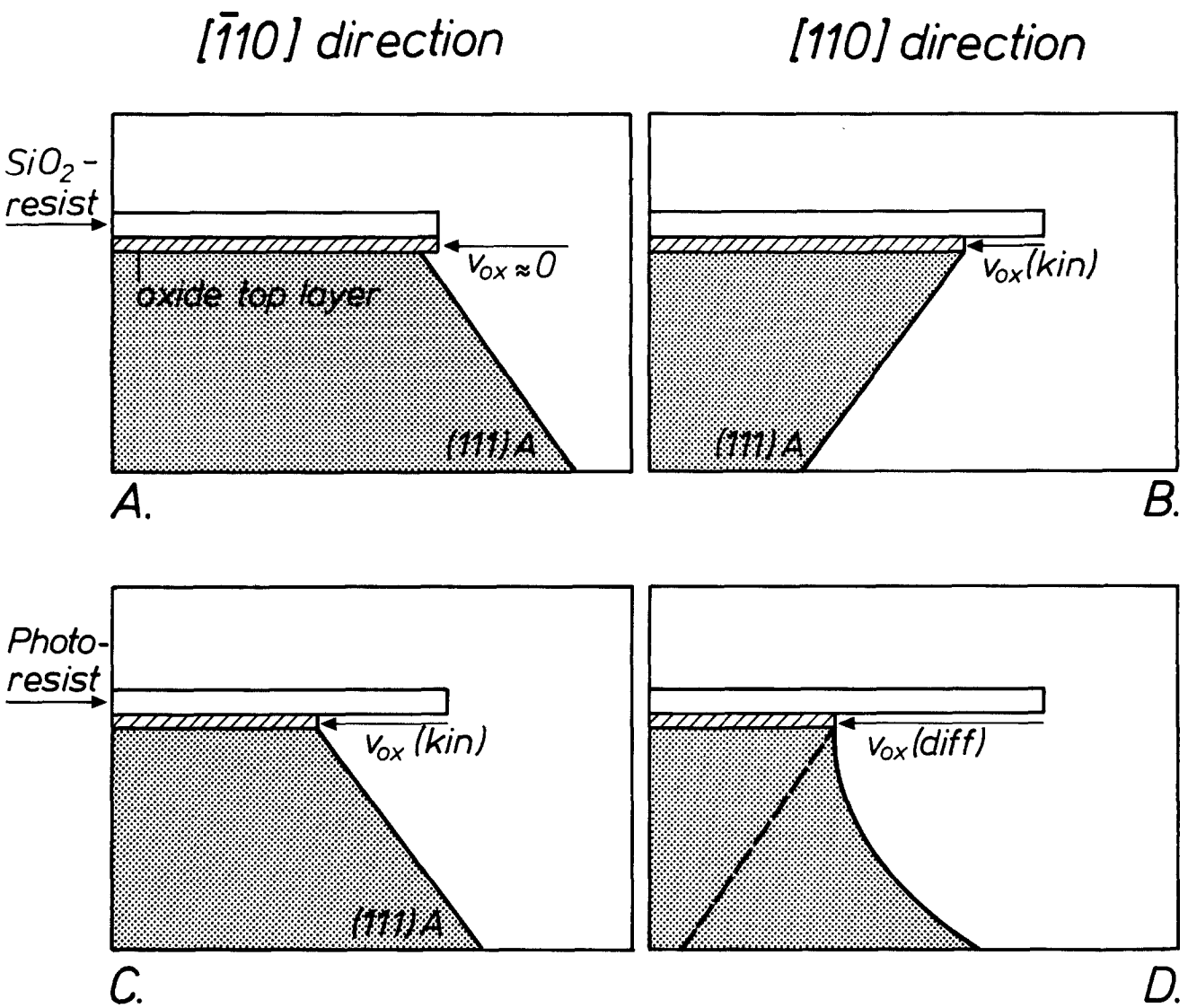


**Fig. 8. Schematic model which shows the influence of an oxide top layer on the shape of the profiles etched in monocrystalline materials (compare with the model for isotropic materials shown in Fig. 7). As described in the text, the lateral etch rate of the oxide layer ($v_{ox}$) is considered to be dependent on whether an $SiO_2$-resist (A and B) or a photoresist (C and D) is used, and on whether the resist is oriented in the [$\bar{1}$10] direction (A and C) or the [110] direction (B and D). This model explains the profile etching results obtained with InP and GaAs (compare with Fig. 4). The relative magnitudes of $v_{ox}$ in the four different cases are represented by the length of the arrows. (111)A represents the (111)In facet in the case of InP.**

ence the microscopic etching kinetics (see Fig. 8A). Consequently, the low etch rate of the (111)In facet in the etching profile of Fig. 4A corresponds exactly to the measured macroscopic etch rate of this facet. This good agreement has already been mentioned. From Fig. 5B we assume that when $SiO_2$ is aligned in the [110] direction, $v_{ox}$ is considerable (see Fig. 8B). Owing to the relatively high etch rate of the native oxide, the (001) surface of the underlying InP substrate is immediately brought into contact with the bromine etchant. Since the etch rate of InP with this crystallographic orientation was found to be controlled by diffusion of $Br_2$ (4), this newly formed surface is instantly dissolved at a high rate until the slowest etching plane, the (111)In facet, is again encountered. In fact, the displacement of this facet is, under these conditions, regulated by the lateral etch rate of the native oxide, as is indicated in Fig. 8B. This explains why the microscopic etch rate of this facet near an $SiO_2$ resist layer can be enhanced significantly as the results of Fig. 2-4 show.

A similar reasoning can, in principle, be applied to explain the etching profiles when a photoresist layer is used as a mask. The faceted profile of Fig. 4C, revealing a high etch rate of the (111)In facet, can be understood if the product of $v_{ox}$ and the etching time corresponds to the underetched distance (see Fig. 8C). Using HBr as "indicator etchant" at 40°C it was concluded from Fig. 6 that $v_{ox}$ is dramatically increased when a photoresist layer is used as mask instead of an $SiO_2$ layer (compare A and B of Fig. 6). Again assuming that bromine accomplishes a similar effect at room temperature, the lateral etch rate of the native oxide might become so high that $v_{ox}$ is no longer kinetically controlled as in Fig. 8A-C, but that the supply of $Br_2$ becomes rate determining (see Fig. 8D). The (111)In facet would then be expected to extend from the oxide edge into the substrate (see the dashed line in Fig. 8D). However, the flux of $Br_2$ species in solution is not sufficient to allow this facet to develop, as both the dissolution rates of the oxide layer and the InP substrate are now controlled by $Br_2$ diffusion. Consequently, a rounded profile is etched (see Fig. 4D and 8D). The shape of these profiles follows closely the described mathematical models (8, 9).

In the model just presented it was assumed that at 20°C only the bromine component in solution dissolves the oxide layer. This was in agreement with the observations that at this temperature etching did not occur in solutions only containing 4.5*M* HBr. However, etching does take place in a 4.5*M* HBr solution at 40°C, as was shown in Fig. 5 and 6. It would therefore be expected that when profile etching experiments are performed in a solution of 0.1*M* $Br_2$, 4.5*M* HBr at higher temperatures that both $Br_2$ and HBr contributed to etching the oxide layer whereas the InP substrate is still only etched by the bromine species. This is indeed what we found experimentally at 40°C, *viz.*, rounded profiles similar to that shown in Fig. 4D and, in

addition, in the region close to the resist layer, lateral etching of the oxide layer. These results are thus in good agreement with the model.

The model proposed to explain the anomalous profile etching results obtained with InP is not restricted to this material. For example, we obtained similar profile etching results with GaAs:(111)Ga exposed facets were etched at 20°C in $Br_2$-HBr solutions when the photoresist was aligned in the [$\bar{1}$10] direction whereas diffusion-controlled rounded profiles were found in the [110] direction (3). This can now be understood by assuming that the microscopic etch rate of the (111)Ga faces is significantly enhanced by an anisotropic native oxide of GaAs.

Clearly, the influence of thin surface layers on the etching properties of monocrystalline materials is more important than has been realized. This opens new and interesting ways of investigating more systematically and regulating more accurately etching profiles. For instance, intentional application to the substrate of a thin surface layer with a different chemical composition could create new possibilities. Since monolayers were found to be sufficiently thick to induce large changes in the etching kinetics (20), chemical surface modification in combination with variations in etchant composition might be successfully applied to regulate etching profiles (21, 22).

## Conclusions

Profile etching experiments were performed on monocrystalline InP in a 0.1*M* $Br_2$, 4.5*M* HBr solution. Bromine is a chemical etchant for InP (3) and is the active etching component in this solution, whereas HBr used in this concentration at moderate temperatures only serves to complex $Br_2$. The results showed that the macroscopic etch rates measured in the previous works can often be used to predict accurately the profile shape.

However, the local etch rates of the (111)In crystallographic facets were found to be significantly enhanced near resist edges in a number of cases, depending on the type and orientation of the resist. A model was proposed to account for the sometimes dramatic changes in profile shape. Thin surface layers, very likely native oxide layers, play a decisive role in this model. Using an "indicator etchant," the lateral etch rate of this oxide was found to be strongly dependent on the crystallographic orientation of the underlying semiconductor substrate. Besides an orientation dependence, the lateral etch rate was also dependent on the nature of the resist; this was attributed to changes induced in the the oxide layer during the different pretreatment processes. Although the exact nature of the oxides has not yet been clarified it was concluded that the microscopic etching kinetics of crystallographic facets are determined by the lateral etch rate of the oxide layer. This model shows that thin surface layers can have a considerable effect on the profile shape near resist edges. A change-over from kinetic to diffusion-controlled profiles as observed in the experiments can be understood with this model.

## Acknowledgments

The author wishes to thank Mr. C. Geenen for making the SEM photographs and Mr. M. Cornelissen for his assistance to the etching experiments. He is also grateful to Professor Dr. J. J. Kelly and Mr. J. E. A. M. van den Meerakker for helpful discussions.

Manuscript submitted March 2, 1990; revised manuscript received July 23, 1990.

*Philips Research Laboratories assisted in meeting the publication costs of this article.*

## REFERENCES

1. *IEEE J. Quant. Electron.*, **QE-19,** G. A. Acket, Editor, p. 897ff. (June 1983).
2. P. H. L. Notten, Ph.D. Thesis, Technical University Eindhoven (1989).
3. P. H. L. Notten, J. E. A. M. van den Meerakker, and J. J. Kelly, "Etching of III-V Semiconductors: An Electrochemical Approach," To be published by Elsevier, Amsterdam (1990).
4. P. H. L. Notten and A. A. J. M. Damen, *Appl. Surf. Sci.*, **28,** 331 (1987).
5. S. Adachi, Y. Noguchi, and H. Kawaguchi, *This Journal*, **129,** 1053 (1982).
6. S. Adachi and H. Kawaguchi, *ibid.*, **128,** 1342 (1981).
7. Y. Mori and N. Watanabe, *ibid.*, **125,** 1510 (1978).
8. H. K. Kuiken, J. J. Kelly, and P. H. L. Notten, *ibid.*, **133,** 1217 (1986).
9. C. Vuik and C. Cuvelier, *J. Comput. Phys.*, **59,** 247 (1985).
10. D. W. Shaw, *J. Cryst. Growth*, **47,** 509 (1979).
11. C. W. Wilmsen, "Physics and Chemistry of III-V Compound Semiconductor Interfaces," Chap. 7, C. W. Wilmsen, Editor, p. 403, Plenum Press, New York (1985).
12. W. C. Dautremont-Smith and D. P. Wilt, Patent Cooperation Treaty (PCT), Int. Publ. Number WO 86/01367, Int. Publ. Date, March 13 (1986).
13. D. T. C. Huo, J. D. Wynn, S. G. Napholtz, F. R. Lenzo, and D. P. Wilt, *This Journal*, **134,** 2850 (1987).
14. D. T. C. Huo, J. D. Wynn, S. G. Napholtz, and D. P. Wilt, *ibid.*, **135,** 2334 (1988).
15. Y. I. Choi, C. K. Kim, and Y. S. Kwon, *IEEE Proc. Pt. I*, **133,** 13 (1986).
16. L. K. White, *This Journal*, **127,** 2687 (1980).
17. S. R. Morrison, "Electrochemistry at Semiconductor and Oxidized Metal Electrodes," Chap. 8, Plenum Press, New York (1980).
18. A. Ourmazd, D. W. Taylor, J. A. Rentschler, and J. Bevk, *Phys. Rev. Lett.*, **59,** 213 (1987).
19. J. J. Kelly and G. J. Koel, *This Journal*, **125,** 860 (1978).
20. O. J. Wimmers, F. J. Touwslager, and J. J. Ponjeé, *ibid.*, **136,** 1769 (1989).
21. J. J. Ponjeé and P. N. T. van Velzen, *Philips Tech. Rev.*, **44,** 81 (1988).
22. J. J. Ponjeé, V. B. Mariott, M. C. B. A. Michielsen, F. J. Touwslager, P. N. T. van Velzen, and H. van der Wel, *J. Vac. Sci. Technol. B*, **8,** 463 (1990).